Nucleon-nucleon correlation effects in the elastic scattering of α particles from ^{11}Li at 26 MeV/nucleon

A. N. F. Aleixo

Instituto de Física, Universidade Federal do Rio de Janeiro, 21945, Rio de Janeiro, Rio de Janeiro, Brazil

C. A. Bertulani

National Superconducting Cyclotron Laboratory, Michigan State University, East Lansing, Michigan 48824

M. S. Hussein

*Nuclear Theory and Elementary Particle Phenomenology Group, Instituto de Física, Universidade de São Paulo,
Caixa Postale 20 516, 01498 São Paulo, São Paulo, Brazil*

The cross section for the elastic scattering of α particles from ^{11}Li at $E_{lab} = 26$ MeV/nucleon is calculated. The single-folding potential plus second-order rescattering correction is used as an optical potential. It is found that the angular distribution is farside dominated. The second-order correction, which contains the short-range correlation effects, merely adds to absorption. Comparison to the $\alpha + {}^{12}$C system is made.

I. INTRODUCTION

Recently, the elastic scattering of different nuclei from ^{11}Li has been calculated [1–3]. The motivation for this interest is connected with the possible encountering of a signature of the neutron halo in the elastic angular distribution and the need of elastic information to study quasi-elastic processes. Experimental programs to investigate these processes are already underway [4]. Further investigation of the elastic scattering involving ^{11}Li is certainly required to better understand the average nuclear interaction.

In the present paper, we extent our study [2] of $p + {}^{11}$Li to the case of $\alpha + {}^{11}$Li. The tightly bound α particle should prove an interesting probe as it represents, at low energies, a heavier charged "nucleon." To what extent the halo of ^{11}Li is sensitive to the size of the impinging particle is a question that can be partly answered by comparing the two systems $p + {}^{11}$Li and $\alpha + {}^{11}$Li at relatively low energies. We take this energy to be $E_{lab} = 26$ MeV/nucleon, since precise data [5] on the elastic scattering of p from α exist and can be used to extract the p-α optical potential. This potential is then used to calculate the α-^{11}Li single-folding optical potential. Since the energy is too low for the usual [6] single-folding approximation to the potential to be valid, we also calculate the second-order contribution which carry important information about nucleon-nucleon short-range correlations in the nucleus.

The plan of the paper is as follows. In Sec. II we give a short summary of the eikonal calculation used in our study. In Sec. III we describe the construction of the $\alpha + {}^{11}$Li optical potential. In Sec. IV we describe the second-order correction to the potential. In Sec. V we show our results for the elastic angular distribution and make a comparison with the $\alpha + {}^{12}$C system. Finally, in Sec. VI we present our concluding remarks.

II. NUCLEUS-^{11}Li SCATTERING AMPLITUDE IN EIKONAL APPROXIMATION

We present in this section the pertinent formulas used in our calculation of the elastic scattering angular distribution. We ignore spin-orbit effects and thus write for the elastic scattering amplitude, $f(\theta)$,

$$f(\theta) = -ik \int_0^\infty db \, bJ_0(qb)(e^{i\chi(b)} - 1) , \qquad (2.1)$$

where $k^2 = 2\mu E_{c.m.}/\hbar^2$, μ is the reduced mass, J_0 is the ordinary Bessel function of order zero, b is the impact parameter, and q is the momentum transfer, $q = 2k\sin(\theta/2)$. The phase $\chi(b)$ contains a nuclear and Coulomb pieces and is given by

$$\chi(b) = \chi_N(b) + \chi_C(b) ,$$

$$\chi_N(b) = -\frac{1}{\hbar v} \int_{-\infty}^\infty dz V_N[(b^2 + z^2)^{1/2}] , \qquad (2.2)$$

$$\chi_C(b) = \frac{2Z_1 Z_2 e^2}{\hbar v} \left[\ln(kb) + \frac{1}{2} E_1\left[\frac{b^2}{r_{m.s.}^2} \right] \right] ,$$

where $E_1(x)$ is the exponential integral, defined as

$$E_1(x) = \int_x^\infty \frac{e^{-t}}{t} dt . \qquad (2.3)$$

The Coulomb phase [6] $\chi_C(b)$ is finite for $b = 0$, yielding

$$\chi_C = \frac{2Z_1 Z_2 e^2}{\hbar v}[\ln(kr_{m.s.}) - C] ,$$

where $C = 0.577\ldots$ is the Euler constant. The constant

$r_{\rm m.s.}$ appearing in the above equations is equal to the root-mean-square radius of ^{11}Li: $r_{\rm m.s.}=3.14$ fm. V_N is the complex nuclear potential and v is the relative velocity. In Sec. III we shall give a detailed discussion of the α-^{11}Li optical potential needed for the calculation of $\chi_N(b)$. In what follows we proceed with our discussion of the general features of the eikonal amplitude (2.1).

Because of the logarithmic divergence of $\chi_C(b)$ with increasing b, it is convenient to write $f(\theta)$ as

$$f(\theta)=-ik\int_0^\infty db\, bJ_0(qb)(e^{i\chi(b)}-e^{i\chi_C(b)})+f_C(\theta)$$

$$=f_N(\theta)+f_C(\theta)\;,\tag{2.4}$$

where $f_C(\theta)$ is given by the usual expression

$$f_C(\theta)=-\frac{\eta}{2k\sin^2\theta/2}\exp\{i[2\sigma_0-\eta\ln(\sin^2\theta/2)]\}\;,\tag{2.5}$$

where $\sigma_0=\arg\Gamma(1+i\eta)$ and $\eta=Z_1Z_2e^2/\hbar v$. We use Eq. (2.4) in our numerical calculation.

It has been proven useful [7] to decompose $f(\theta)$ into its near- and farside components. This is accomplished by first writing the Bessel function as

$$J_0(qb)=\tfrac12[H_0^{(1)}(qb)+H_0^{(2)}(qb)]\;,\tag{2.6}$$

where $H_0^{1(2)}(qb)$ is the Hankel function of order zero and first (second) type. Asymptotically, these functions behave as

$$H_0^{1(2)}\to\left[\frac{2}{\pi x}\right]^{1/2}\exp\left[\pm i\left[x-\frac{\pi}{4}\right]\right]\quad\text{for }x\to\infty\;.\tag{2.7}$$

With (2.6) the amplitude $f(\theta)$ can be written as

$$f(\theta)=f_{\rm near}(\theta)+f_{\rm far}(\theta)\;,\tag{2.8}$$

where $f_{\rm near}(\theta)[f_{\rm far}(\theta)]$ is given by (2.1) with $J_0(qb)$ replaced by $H_0^{(2)}(qb)/2\;[H_0^{(1)}(qb)/2]$.

In the limit when $\chi_C(qb)$ is negligible and $\chi_N(qb)$ is pure imaginary (no refraction) it is easy to see that the following relation holds [7]:

$$f_{\rm near}(\theta)=-f_{\rm far}^*(\theta)\;.\tag{2.9}$$

The above results in an angular distribution that exhibits simple black-disk Fraunhofer diffraction patterns since the near and far amplitudes are equal in magnitude. In our case of $\alpha+^{11}$Li one expects strong refractive effects arising from both the Coulomb and nuclear interactions. In particular, the elastic scattering of α particles from several targets have clearly established the phenomenon of nuclear rainbow, a situation characterized by the dominance of the farside component over the nearside. At very small angles one always encounters the opposite situation, namely $f_{\rm near}/f_{\rm far}\gg1$, owing to the influence, on the angular region, of Coulomb repulsion which affects mostly $f_{\rm near}$.

To better understand the above features, it is useful to rely on the stationary phase method, more commonly applied to the partial-wave expansion of $f(\theta)$. Here we

summarize the major findings of Ref. [7] involving the stationary phase evaluation of the eikonal amplitude, Eq. (2.1).

Whenever the phase $\chi(b)$ is large, which is expected to the case in our system, the stationary-phase method becomes applicable. We obtain for the near and far contributions the following:

$$f_{\rm near}(\theta)\approx-\frac{ikb_N}{2}\left[\frac{2\pi i}{|\chi''(b_N)|}\right]^{1/2}$$

$$\times e^{i\chi(b_N)}H_0^{(2)}[q(b_N)b_N]\;,\tag{2.10a}$$

$$f_{\rm far}(\theta)\approx-\frac{ikb_F}{2}\left[\frac{2\pi i}{|\chi''(b_F)|}\right]^{1/2}$$

$$\times e^{i\chi(b_F)}H_0^{(1)}[q(b_F)b_F]\;,\tag{2.10b}$$

where $b_{N(F)}$ are determined from the stationary-phase conditions

$$\pm q=\frac{d}{db}\chi(b)|_{b_{N(F)}}\;,\tag{2.11}$$

which, when Eq. (2.2) is used, gives

$$\pm q=-\frac{1}{\hbar v}\int_{-\infty}^\infty dz\frac{b}{(b^2+z^2)^{1/2}}\frac{dV_N[(b^2+z^2)^{1/2}]}{d(b^2+z^2)^{1/2}}$$

$$+\frac{2Z_1Z_2e^2}{\hbar v}\frac{1}{b}\;.\tag{2.12}$$

Notice that the Coulomb term represents the high energy limit of the usual formula $2\tan(\eta/kb)$. The easiest way to appreciate the above equation is to consider, in the application of the stationary phase method, only the real part of the nuclear phase $\chi_N(b)$, and, accordingly, the integrand in Eq. (2.12) is real and positive at the energies considered here. This allows real solutions of the above equations to correspond to scattering in the illuminated region. Complex solutions would then be associated with the classically forbidden region.

A simple analytical evaluation of Eq. (2.12) is normally not possible when a Woods-Saxon potential is used for V_N. Approximate formulas, however, can be obtained in the acceptable limit of small diffuseness (compared to the radius). We obtain

$$\pm q=\frac{k}{E}\sqrt{2b}\left[\frac{V_0}{\sqrt{a_r}}g'(x)\right],\quad x=\frac{b-R}{a_r}\;,\tag{2.13}$$

where U_0 is the strength (positive) of the assumed Woods-Saxon real potential. a_r is its diffuseness and $g(x)$ is a function evaluated in Ref. [7] and is given by

$$g(x)=\bar V-\frac{\mu}{2\bar V}(1-e^{-2\bar V^2/(\mu+1)})$$

$$+\frac{e^{\mu/2}}{\bar V\sqrt{2\mu}}{\rm erfc}(\sqrt{\mu/2})\sqrt{\pi/2}\;,\tag{2.14}$$

where

$$\mu = \exp\left[\frac{b-R}{a_r} + \bar{V}^2\right]$$

and $\bar{V}$ is the solution of the equation

$$\bar{V} = \tfrac{1}{2}\coth[\tfrac{1}{2}(x + \bar{V}^2)] \ . \tag{2.15}$$

For $-x \gg 1$, $\bar{V} \approx \sqrt{-x}$ and one obtains, for small b,

$$g(x) = \sqrt{-x} - \frac{1 - e^x}{2\sqrt{-x}}$$
$$+ \frac{e^{-x/2(1-x)}}{\sqrt{2}(1-x)}\sqrt{\pi/2}\,\text{erfc}\left[\frac{-x}{2(1-x)}\right]^{1/2} \ . \tag{2.16}$$

On the other hand, for large b, $x > 0$ and one finds here $\bar{V} \approx 1/\sqrt{2}$ and

$$g(x) \approx \sqrt{2/e}\,e^{-x} \ . \tag{2.17}$$

Therefore, a simple formula which can be used to obtain b_N is

$$q = -\frac{k}{E}(2b_N\sqrt{2/e})^{1/2}\frac{V_0}{\sqrt{a_r}}e^{-(b_N-R)/a_r} + \frac{2\eta}{b_N} \ . \tag{2.18}$$

The above equation clearly gives two solutions for b_N. One corresponds to predominantly Coulomb scattering and the other, nuclear scattering. The limiting value of q above, with no real solution for b_N, represents the rainbow momentum transfer and is obtained from the condition $dq/db_N = 0$ or

$$q_r = \left|-\frac{a_r}{b_N^r} + 1\right|\frac{2\eta}{b_N^r} \ . \tag{2.19}$$

At $E_{\text{lab}} \approx 100$ meV for α scattering, one has a small η and a value of b_N^r which is equal to or larger than the sum of the radii $R_\alpha + R_{^{11}\text{Li}}$. This shows that q_r is rather small. In fact, our detailed numerical calculation to be presented in Sec. IV demonstrates that q_r is close to zero. This indicates that the $q > q_r$ scattering region is predominantly farsided and dominated by the nuclear attraction at smaller b's. Furthermore, one anticipates seeing greater sensitivity to the details of the nuclear potential in $f(\theta)$, and accordingly corrections to the double- or single-folding potentials arising from higher-order effects (correlations) can be tested. We now turn to a detailed discussion of V_N for $\alpha + {}^{11}\text{Li}$.

III. THE OPTICAL POTENTIAL FOR
THE $\alpha + {}^{11}\text{Li}$ SYSTEM

In this section we discuss the $\alpha + {}^{11}\text{Li}$ interaction potential needed for our elastic scattering calculation. Since
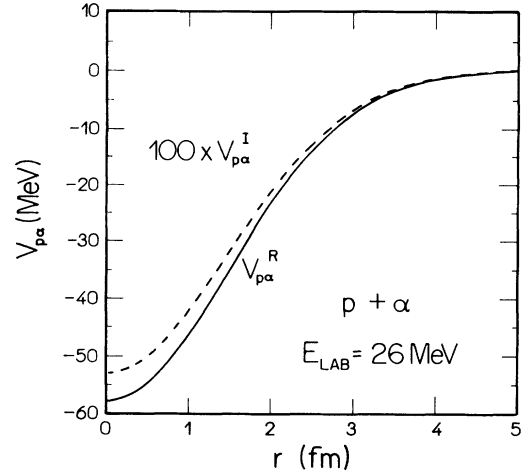

FIG. 1. Imaginary part (dashed curve) and real part (solid curve) of the optical potential for $p + \alpha$ scattering.

no empirical potential is available, we have to rely on appropriate theory. The most natural theoretical framework is based on the multiple scattering theory recently reviewed for heavy ion scattering in Ref. [6]. At the low energies considered here, $E_{\text{lab}} = 26$ MeV/nucleon, medium corrections have to be properly incorporated. Furthermore, higher-order scattering effects, which contain short-range correlation effects, are also potentially important. Instead of using as a leading term the medium modified "$t\rho\rho$ potential" we think it is more appropriate to use available experimental data on the elastic scattering of protons from α and then use a single folding with the ^{11}Li matter distribution [8]. In this way it becomes easier to investigate the effect of the halo neutrons. We then write for the first-order potential
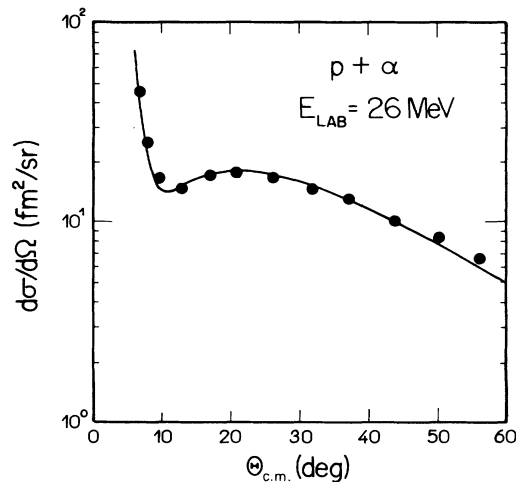

FIG. 2. Elastic scattering cross section for the system $p + \alpha$ at 26 MeV/nucleon. Data are from Ref. [5]. Solid curve is a calculation using the potential of Fig. 1 (see text for details).
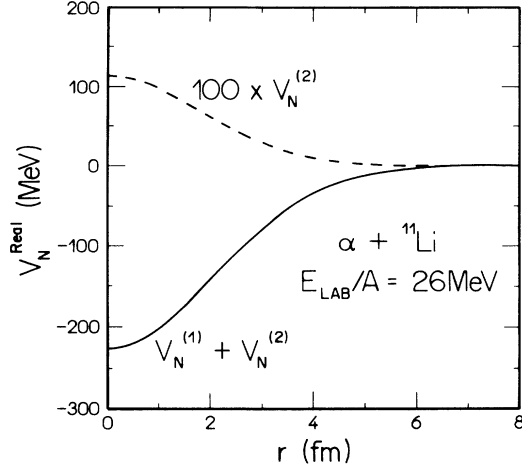
FIG. 3. Real part of the second-order correction for the $\alpha+^{11}$Li optical potential (dashed line). The solid line is the sum of the first- and second-order potentials [Eqs. (3.1) and (3.3)].

$$V_N^{(1)}(\mathbf{r}) = \int d^3r' V_{p\alpha}(\mathbf{r}-\mathbf{r}')\rho_{\mathrm{Li}}(\mathbf{r}') \ . \tag{3.1}$$

The potential extracted from the elastic scattering of protons from α particles at 26 MeV/nucleon laboratory energy is shown in Fig. 1. The elastic scattering data of Ref. [5] are shown in Fig. 2. The core neutrons and protons in ^{11}Li certainly feel a potential which is slightly different from $V_{p\alpha}$ because of medium effects. On the other hand, the halo neutrons in the $1p_{3/2}$ levels, being very loosely bound, should behave almost as freely. So, the "experimental" $V_{p\alpha}$ of Fig. 1 should be quite adequate in describing their interaction with α.

In principle, a better treatment for the $\alpha+^{11}$Li interaction would be taking a double-folding potential for the ^{9}Li$+\alpha$ interaction and a single-folding potential for the interaction of the halo:

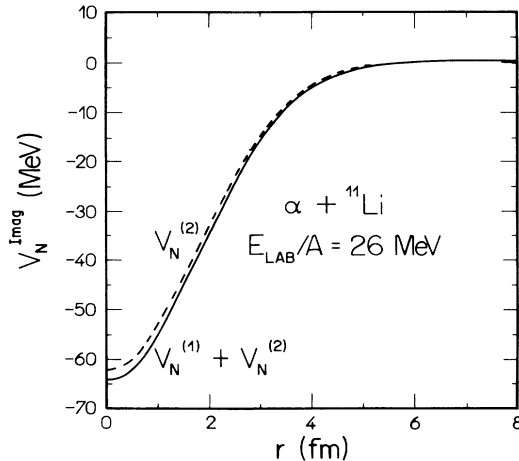$$V_N^{(1)} = \langle t_{NN} \rangle \int d^3r' \rho_{9_{\mathrm{Li}}}(\mathbf{r}-\mathbf{r}')\rho_\alpha(\mathbf{r}')$$
$$+ \int d^3r' V_{n\alpha}(\mathbf{r}-\mathbf{r}')\rho_{2n}(\mathbf{r}') \ , \tag{3.2}$$

where $\langle t_{NN} \rangle$ is the medium-modified nucleon-nucleon t-matrix calculated in the forward direction. We have compared Eqs. (3.1) and (3.2), and found the difference in the real and imaginary parts, less than 10%. Thus, for simplicity we shall in the following use Eq. (3.1) for $V_N^{(1)}(r)$.

In Ref. [6] a detailed discussion of second-order potential which contains the nucleon-nucleon short-range effects has been given. Within a single-folding framework, this potential, which we denote by $V_N^{(2)}(r)$, is given by

$$V_N^{(2)} = -\frac{ik_\alpha}{2E_\alpha}R_{\mathrm{corr}} \int [V_{p\alpha}(\mathbf{r}-\mathbf{r}')]^2\rho_{\mathrm{Li}}(\mathbf{r}')d^3r' \ , \tag{3.3}$$

where R_{corr} is the correlation length and is generally taken to be -0.411 fm and $k_\alpha(E_\alpha)$ is the wave number (energy) of the α particle. In Figs. 3 and 4 we show the real and the imaginary part of $V_N^{(2)}(r)$ and the sum $V_N^{(1)}(r)+V_N^{(2)}(r)$. The effect of $V_N^{(2)}(r)$ is quite noticeable.

IV. RESULTS AND DISCUSSIONS

Before we show our results for the angular distribution of the elastic scattering of the system $\alpha+^{11}$Li at $E_{\mathrm{lab}}=26$ MeV/nucleon, we first discuss the nature of the refraction in this system, exemplified by the momentum transfer function $q(b)$ of Eq. (2.12) (the right-hand side of this equation). In Fig. 5 we show $q(b)$ for $\alpha+^{11}$Li (solid

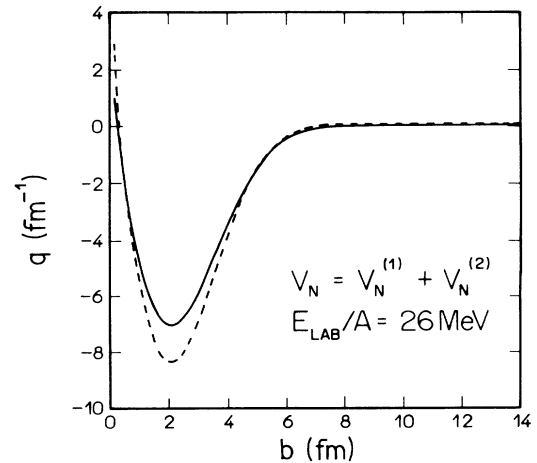FIG. 4. Same as Fig. 3, but for the imaginary part of the potentials.

FIG. 5. Classical momentum transfer [Eq. (2.11)] as a function of impact parameter for the reactions $\alpha+^{11}$Li (solid line) and $\alpha+^{12}$C (dashed line).
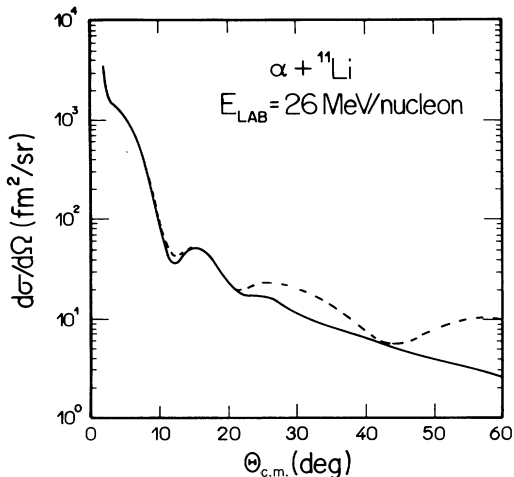
FIG. 6. Elastic cross section for the system $\alpha + {}^{11}$Li at 26 MeV/nucleon. The dashed line was calculated with the first-order optical potential. The solid line includes the contribution of the second-order potential.

FIG. 8. Comparison between the elastic cross section for the systems $\alpha + {}^{11}$Li and $\alpha + {}^{12}$C at 26 MeV/nucleon. Both calculations include the contribution of the second-order potential.

line) calculated with $V_N^{(1)}$ and with $V_N^{(1)} + V_N^{(2)}$. Very little change is seen when the second-order potential is added. However, the absorption content of $V_N^{(1)} + V_N^{(2)}$ is quite different from $V_N^{(1)}$, as will be seen next. For comparison we also exhibit (dashed curve) $q(b)$ for $\alpha + {}^{12}$C at the same energy ($E_{lab} = 26$ MeV/nucleon). Again a small effect is seen to arise from $V_N^{(2)}$. Notice that the nuclear rainbow (the dip at negative q) is at a larger negative q in ^{12}C than in ^{11}Li. The large-b behavior of $q(b)$ is slightly different in the two systems.

The cross section for $\alpha + {}^{11}$Li calculated with $V_N^{(1)}$ and $V_N^{(1)} + V_N^{(2)}$ is shown in Fig. 6. We see here a drastic change in behavior at larger angles ($\theta > 10°$), which arises from the different absorption content in the two potentials. Figure 7 is the result of the same calculations, but for the system $\alpha + {}^{12}$C. Again for comparison, we show
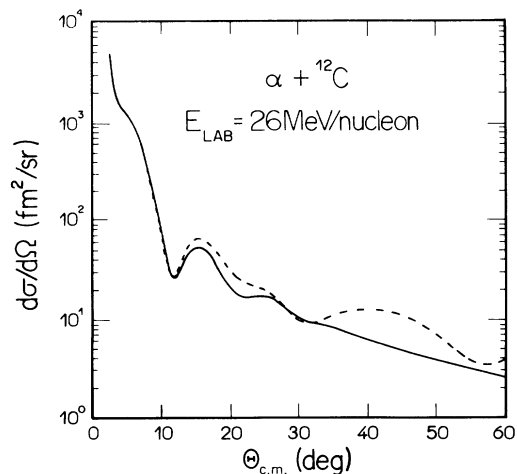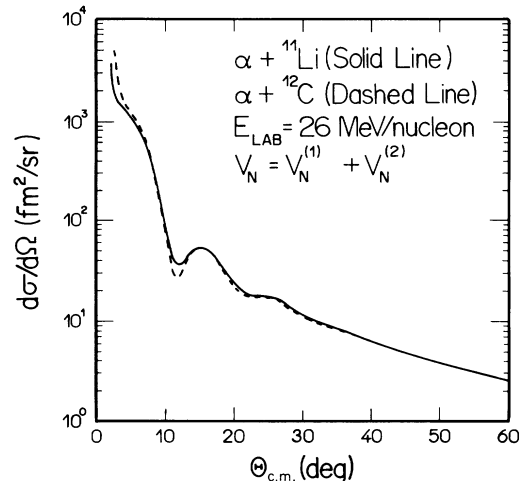
in Fig. 8 the $\alpha + {}^{12}$C as compared to the $\alpha + {}^{11}$Li results. This figure implies stronger refraction is seen in $\alpha + {}^{11}$Li, which corroborate the findings of Satchler et al. [1] on the ^{11}Li + ^{12}C systems.

To better understand the nature of the angular distribution, we show in Fig. 9 the near and far contributions to $d\sigma/d\Omega$ for both $V_N^{(1)}$ and $V_N^{(1)} + V_N^{(2)}$. It is clear that, in both cases, the angular distribution is farside dominated, indicating great sensitivity to the nuclear potential at shorter distances. However, the oscillations (Airy) in the farside amplitude are washed out when $V_N^{(1)} + V_N^{(2)}$ is used. This shows that $V_N^{(2)}$ contributes basically to absorption in such a way as to damp the contribution to $f_{far}(\theta)$ arising from the inner stationary phase point. This feature is common to both $\alpha + {}^{11}$Li and $\alpha + {}^{12}$C.

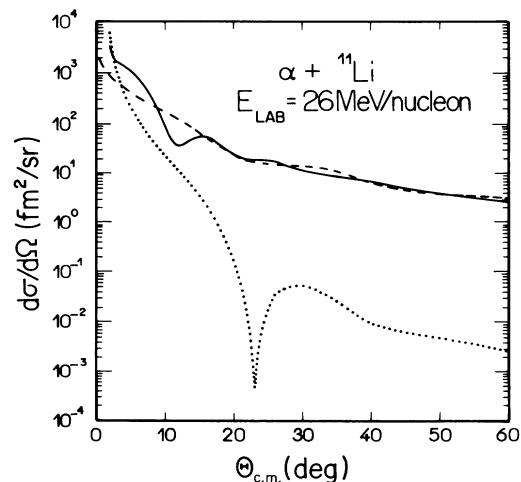FIG. 7. Same as in Fig. 6, but for the system $\alpha + {}^{12}$C at 26 MeV/nucleon.

FIG. 9 Near- (dotted curve) and farside (dashed curve) contribution to the elastic scattering cross section (solid) for the system $\alpha + {}^{11}$Li at 26 MeV/nucleon.

V. CONCLUSIONS

In this paper we have investigated the elastic scattering of α particles from ^{11}Li at $E_{lab} = 26$ MeV/nucleon. Comparison to the system $\alpha + {}^{12}$C at the same laboratory energy indicate more refractive effects in $\alpha + {}^{11}$Li as compared to $\alpha + {}^{12}$C. This is in agreement with the finding of Satchler *et al.* [1] on the system ^{11}Li + ^{12}C at slightly higher energy. We also investigated the influence of NN short-range correlations of the potential through the calculation of the second-order potential. We found that this potential contributes little to refraction but increases absorption.

[1] G. R. Satchler, K. W. McVoy, and M. S. Hussein, Nucl. Phys. **A522**, 621 (1991).

[2] A. N. F. Aleixo, C. A. Bertulani, and M. S. Hussein, Phys. Rev. C **43**, 2722 (1991).

[3] Y. Hirabayashi, S. Funada, and Y. Sakuragi, Contribution to the Symposium on Structure and Reactions of Unstable Nuclei, Niigata, Japan, 1991 (unpublished), p. 23.

[4] J. Kolata, private communication.

[5] D. J. Plummer *et al.*, Nucl. Phys. **A174**, 193 (1971).

[6] M. S. Hussein, R. A. Rego, and C. A. Bertulani, Phys. Rep. **201**, 279 (1991).

[7] M. S. Hussein and K. W. McVoy, Prog. Part. Nucl. Phys. **12**, 103 (1984); B. V. Carlson, M. P. Isidro Filho, and M. S. Hussein, Phys. Lett. **154B**, 89 (1985).

[8] G. F. Bertsch, B. A. Brown, and H. Sagawa, Phys. Rev. C **39**, 1154 (1989).